Δ -based composite models for calculating x-ray absorption and emission energies Θ

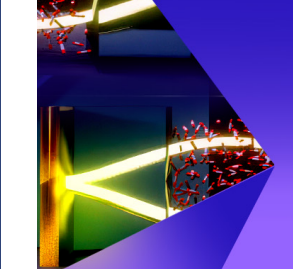
Abdulrahman Y. Zamani ■ (i); Hrant P. Hratchian (ii)



J. Chem. Phys. 159, 224109 (2023) https://doi.org/10.1063/5.0178052







The Journal of Chemical Physics

Special Topic: Polaritonics for Next Generation Materials

Submit Today





Δ-based composite models for calculating x-ray absorption and emission energies

Cite as: J. Chem. Phys. 159, 224109 (2023); doi: 10.1063/5.0178052 Submitted: 26 September 2023 • Accepted: 16 November 2023 • Published Online: 12 December 2023







Abdulrahman Y. Zamania 🕩 and Hrant P. Hratchian 🕩





AFFILIATIONS

Department of Chemistry and Biochemistry and Center for Chemical Computation and Theory, University of California, Merced, California 95343, USA

a) Author to whom correspondence should be addressed: azamani2@ucmerced.edu

ABSTRACT

A practical ab initio composite method for modeling x-ray absorption and non-resonant x-ray emission is presented. Vertical K-edge excitation and emission energies are obtained from core-electron binding energies calculated with spin-projected ΔHF/ΔMP and outer-core ionization potentials/electron affinities calculated with electron propagator theory. An assessment of the combined methodologies against experiment is performed for a set of small molecules containing second-row elements.

Published under an exclusive license by AIP Publishing. https://doi.org/10.1063/5.0178052

I. INTRODUCTION

Spectroscopic analysis using x-ray and electron sources provides rich information on the characteristic properties of materials. ^{1–3} Techniques, such as x-ray photoelectron spectroscopy (XPS), probe the valence and core-level energy signatures for a local chemical environment via ionization. Core-excited states are accessed with x-ray absorption spectroscopy (XAS) and innershell electron energy loss spectroscopy (ISEELS). Non-resonant x-ray emission spectroscopy (XES) measures the radiative decay of an outer-core electron into a core hole formed upon ionization. Advances in x-ray techniques such as these have seen ancillary development of theoretical methods for interpreting core spectra, which is critical for studying ultrafast chemical reactivity and

Historically, quantum chemical methods for modeling coreionization often used the difference of self-consistent-field solutions (Δ SCF) for the N and N-1 states (where N is the number of electrons).^{8,9} Early computation of x-ray emission energies used a two-step model involving the difference between the detachment energy, or ionization potential (IP), of the K-shell electron and the valence IPs of the neutral species.¹⁰ The formula for the non-resonant emission energy \mathcal{E}_X is

$$\mathcal{E}_X = \mathrm{IP}_{\mathrm{core}} - \mathrm{IP}^f, \tag{1}$$

where IP^f is the energy to reach a particular final state configuration in which a higher occupied orbital reoccupies the ionized core (see Fig. 1). Specialized methods using equation of motion coupled cluster singles and doubles (EOM-CCSD), algebraic diagrammatic construction (ADC) schemes, GW + BSE, and time-dependent density functional theory (TD-DFT) have been applied to studies of XES. 11-14 Similarly, the x-ray absorption energy is obtained through the difference of IPcore and the electron affinity (EA) of a virtual orbital in the core-ionized system. The excitation energy ω_X is

$$\omega_X = \mathrm{IP}_{\mathrm{core}} - \mathrm{EA}_{\mathrm{core}}^f,$$
 (2)

where EA_{core} is the energy to attach an electron, in the presence of the core-hole, to an orbital that is occupied in the final neutral excited state configuration (see Fig. 2). This is analogous to approaches based on the static-exchange approximation (STEX) where excitation energies are estimated through EAs obtained from configuration interaction singles (CIS) calculations with an optimized core-hole reference. 15-17 Recent extensions of STEX to time-dependent density functional theory (TD-DFT) are able to produce highly accurate K-edge excitation energies.¹⁸ Related approaches for computing core excitation and ionization energies from coupled cluster (CC) theory, such as electron attachment equation-of-motion (EA-EOM-CC) and Δ-based CC

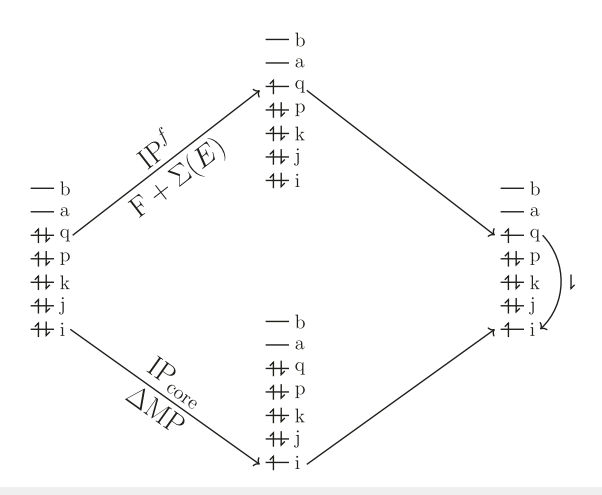


FIG. 1. Model schematic for non-resonant XES with a closed shell reference.

methods, are also shown to be very accurate and amenable to systematic improvements. $^{19\mbox{--}23}$

It is well known that Δ SCF captures the orbital relaxation (ORX) effects that accompany the formation of the core-hole state. This reasoning supports its viability for obtaining good estimates for IP_{core}, which can be further refined with Møller–Plesset (MP) perturbation theory. The values for outer-valence IPs in addition to EAs of unoccupied levels can be accurately computed with one-particle Green's function methods. ^{28–31}

In this study, we propose and examine composite models that incorporate Δ SCF and Δ MP methods with self-energy $\Sigma(E)$ corrections to the eigenvalues of the Fock operator F. The computational protocol for obtaining representative single-reference solutions is delineated and results for vertical K-edge excitation and emission energies are presented.

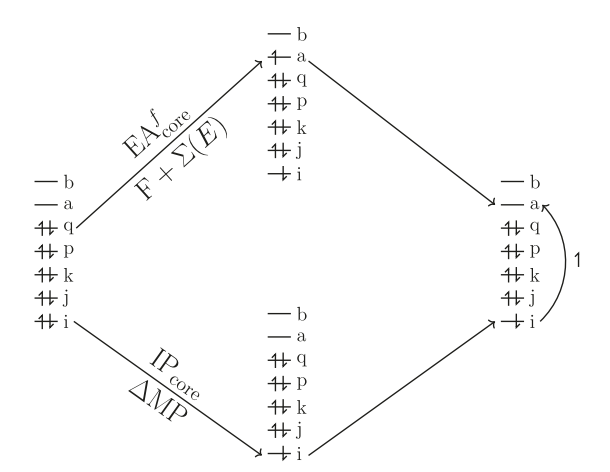


FIG. 2. Model schematic for XAS with a closed shell reference.

II. METHODS

In this section, we describe the individual procedural components of the composite models. These include SCF reference calculations, computation of core-hole intermediates, spin projection schemes, determination of IPs and EAs with a post-SCF response method, and additional capabilities for estimating emission intensities.

The value of IPcore can be approximated by subtracting the N and N-1 total energies obtained from Hartree-Fock (HF) calculations. The representative core-hole state can be generated by applying projection operators or level-shifting in a modified SCF In this work, the non-Aufbau solutions are conalgorithm.3 verged using the projected initial maximum overlap method.³⁴ To include correlation effects in the initial neutral the final ionized states not contained in Δ HF, a series of Δ MPn (n = 2, 2.5, 3) methods are employed. Numerical issues may arise when using corehole reference determinants with MP expansions. Certain orbital indices coupled to the core hole can lead to near-zero denominators and instabilities reflected in divergent MP energies. Procedures described in recent literature³⁵ are adopted to mitigate this effect. This involves removing orbital indices contributing to second-order energy denominators below a 0.02 a.u. threshold.

For ionization in closed-shell species, the unrestricted Hartree–Fock (UHF) result for the core-hole doublet typically exhibits minor spin polarization due to the spatial contraction of the electronic structure influenced by the increased effective nuclear charge. The spin contamination is typically low but not always negligible. Often, conceptual deficiencies of broken-symmetry solutions can be remedied with spin projection. Spin-projected energies are calculated perturbatively through a composite Hamiltonian of under a class of approximate projection-after-variation (PAV) methods. The spin-projected methods are denoted as PUHF and PUMP*n*.

Electron propagator theory (EPT) is a formalism for the oneelectron Green's function that provides a foundation for the direct calculation of IPs, EAs, and Dyson orbitals from first principles.⁴¹ Systematic improvements to self-energy approximations have been formulated and thoroughly assessed.⁴² Its advantage as a correlated one-electron theory is reflected in the inclusion of important many-body interactions that follow a physical change in particle number while still retaining the intuitive utility of orbital concepts routinely used in molecular quantum chemistry. The renormalized partial third-order (P3+) method is a diagonal quasiparticle approximation for accurate determination of vertical IPs and EAs.⁴⁶ The overestimation of correlation contributions typical of second-order corrections and exaggerated final-state relaxation effects offered at partial third-order are ameliorated with P3+. P3+ is also selected as an optimal, cost-effective approach for its modest arithmetic bottleneck of $\mathcal{O}(O^2V^3)$ (where O and V give the number of occupied and virtual molecular orbitals (MOs)) and for its reduced storage requirements for generating the largest transformed integral subset of type $\langle OV||VV\rangle$ needed to calculate IPs. Symmetryadapted implementations can then accelerate the time-to-solution for each pole search. The probability factors or pole strengths (PS) that accompany the quasiparticle corrections are the norms of the Dyson orbitals. A PS above 0.85 indicates that the Dyson orbital is dominated by a single canonical MO and that qualitative one-electron concepts for interpreting the $N\pm 1$ states hold. 47,48

Since core emission spectra typically resemble the photoelectron spectrum of the valence electrons that will undergo deexcitation, intensities or photoionization cross sections can be inferred from the proportional PS values. Relative emission intensities can also be obtained with transition dipole moments evaluated in the frozen orbital approximation. $^{49-51}$ From the assumption that the core orbital is highly localized and that de-excitations involve valence MOs built from local atomic contributions, population analysis of the 2p character in the neutral-state valence MOs can be used to approximate the relative intensities for one-particle corehole decay for second-row elements. $^{52-54}$ The squares of the 2p components of the MO coefficients are summed over the atomic center(s) to reconstruct main-line non-resonant emission spectra for N_2 , H_2O , and C_2H_4 .

III. NUMERICAL RESULTS AND DISCUSSION

Two sets of molecules are examined for the evaluation of \mathcal{E}_X . The first test set contains results for C, N, O, and Ne K-edge. Δ PUHF and Δ PUMPn values for IPcore are computed using the aug-cc-pCVTZ basis with modification. For hydrogen, the cc-pVTZ basis is used. For post-SCF denominator control in this set, f-functions are removed to reduce or remove instances of high-energy virtual MOs spawned from atomic orbitals with high angular momentum. The second group of molecules is composed of fluoromethanes, for which IPcore is computed using the full aug-cc-pCVTZ basis set. The IPcore estimates for a selection of molecules from the first set, along with H₂O₂, are used for evaluations of ω_X . When applying Δ -based methods for ionizations of symmetry-equivalent atomic cores, an effective core potential (ECP) is applied to all other atoms except the target site and any hydrogen atoms.

The average percent deviation of $\langle S^2 \rangle_{\text{UHF}}$ for the entire set of core-hole doublets is 17%. The two core-hole spin channels for NO consist of a singlet and triplet with $\langle S^2 \rangle_{\text{UHF}}$ values of 1.241 and 2.578, respectively. Spin contamination is removed through successive annihilation up to S+4 with projected MP.

Relativistic effects are incorporated using methodologies previously reported in the literature. Specifically, molecular relativistic corrections for C, N, O, and F are 0.05, 0.1, 0.2, and 0.35 eV, respectively.⁵⁵ The atomic relativistic correction for Ne is 1.2 eV.^{56,57}

Propagator calculations for IP f using the P3+ method on neutral species are performed with the cc-pVTZ basis set. Many transitions beyond the lowest unoccupied orbital exhibit Rydberg character and increasing orbital angular momentum l—requiring additional diffuse and polarization functions for accurate excitation energies. The d-aug-cc-pV6Z basis truncated at l = 3 is then used for computing bound-state (positive) EA $_{\rm core}^f$ values with P3+. This approach is chosen for consistency and as an expedient approach toward customized basis set saturation. The core-hole reference for computing EAs is simulated with a Z + 1 model where the number of electrons is conserved and the atomic number Z of the target atom is increased by one. When the core orbitals of interest are delocalized by symmetry, the +1 charge is distributed evenly among equivalent atoms.

Geometries are obtained from the NIST CCCBDB⁶⁰ and Ranasinghe *et al.*⁶¹ Structures are optimized at the CCSD(T)/aug-cc-pVTZ level except CF₄, which is optimized at the ω B97X-D/aug-cc-pVTZ level of theory. Δ PUHF, Δ PUMPn, and EPT calculations were performed with a development version of the Gaussian suite of programs.⁶² Integral symmetry with Abelian groups is used when applicable. Basis sets are acquired from the Basis Set Exchange.⁶³

Experimental values for non-resonant valence-to-core emission energies available in the literature are reported from direct XES measurements or inferred from differences in photoelectron spectra. Observed excitation energies are taken from XAS and ISEELS experimental data. Experimental emission spectra are traced using WebPlotDigitizer.⁶⁴

Vertical emission energies at the C, N, O, and Ne K-edge are reported in Table I. The average pole strength for this set PS_{ave} is 0.90 which suggests that the canonical MOs are a good approximation for the Dyson orbitals. The lowest or minimum value PS_{min} for this set is 0.84 and is reflected in low PS values corresponding to inner-valence electron detachments in N2O and C2H4. It is not unexpected that ionizations from inner-valence orbitals involve many-body effects of quantitative importance even though a single MO can be designated in the qualitative picture of electron detachment. Spin projection of the UHF states ensures that the total energies used to determine IP_{core} correspond to eigenstates of S^2 . The errors for Δ PUHF with P3+ imply that additional electron correlation effects can be important in the initial state, core-hole ion, final state, or all of these. $\Delta PUMPn$ (n = 2, 2.5, 3) should provide similar estimates for IP_{core} for localized core orbitals. This is evident in the consistent measure of errors for each method. We briefly note that NO has an open-shell ground state with two core-ionization channels: $^3\Pi$ and ¹Π. A removal of a down-spin β electron in the N_{1s} orbital yields a triplet final-state configuration ${}^3\Pi$, whereas a removal of an up-spin α electron results in the singlet ${}^{1}\Pi$. Valence-to-core decay in either scenario leads to even more electronic states and complex spectral features.

 \mathcal{E}_X results for the set of fluoromethanes are given in Table II. Similar assessments for results featured in Table I can be made for the performance of each composite method here. PS_{min} is 0.84 as well and corresponds to the $2t_2$ detachment in CF₄.

Vertical core-excitation energies at the C, N, O K-edge are displayed in Table III. Beyond transitions into the lowest unoccupied π^* or σ^* lie a series of Rydberg states of increasing principal and azimuthal quantum numbers. A higher lying orbital is diffuse and to attach an electron requires a sufficient basis set describing its large radial extent. High-energy Rydberg states are largely independent of the occupied electronic structure and appear quasi-hydrogenic. A PS_{ave} that is effectively equal to 1 again suggests that the Dyson orbital is sufficiently described by the canonical MO and the computed value for EA_{core}^f should also be reasonable. In relation to this, the excited-state Rydberg series can also be directly characterized with molecular quantum defect analysis and EPT. 65,66 The results for C, N, O K-edge excitations are comparable to those of emission in that the errors for $\Delta PUMPn$ are less than 1 eV. $\Delta PUHF$ still confers a mean-absolute-error (MAE) and root-mean-squareerror (RMSE) that are ~1 eV. The computational results for vertical core-to-valence and valence-to-core transitions indicate that both self-energy corrections and Δ -driven recovery of core-hole ORX are jointly modeling the correct physics.

TABLE I. Vertical C-N-O-Ne K-edge emission energies \mathcal{E}_X computed with projected \triangle MPn and EPT [P3+].

Molecule	Core	Orbital	$\Delta PUHF [P3+]$	$\Delta PUMP2 [P3+]$	ΔPUMP2.5 [P3+]	ΔPUMP3 [P3+]	Exp.
	С	5σ	281.1 (-1.0)	282.5 (0.4)	282.4 (0.3)	282.4 (0.3)	282.194
CO	С	1π	278.3 (-0.9)	279.7 (0.5)	279.7 (0.5)	279.6 (0.4)	279.2^{94}
CO	O	1π	524.3 (-1.2)	525.9 (0.4)	525.7 (0.2)	525.5 (0.0)	525.5^{94}
	О	4σ	521.5 (-1.1)	523.2 (0.6)	523.0 (0.4)	522.8 (0.2)	522.694
N_2	N	$3\sigma_g$	393.1 (-1.2)	395.2 (0.9)	394.9 (0.6)	394.5 (0.2)	394.3 ⁹⁴
1N2	N	$1\pi_u$	391.6 (-1.3)	393.7 (0.8)	393.3 (0.4)	393.0 (0.1)	392.994
	N(S=0)	2π	402.7 (0.6)	403.0 (0.9)	403.0 (0.9)	403.0 (0.9)	402.1^{94}
NO	N(S=1)	5σ	392.8 (-1.0)	394.8 (1.0)	394.6 (0.8)	394.4 (0.6)	393.8 ⁹⁴
	N(S=0)	5σ	394.8 (1.3)	395.1 (1.6)	395.1 (1.6)	395.1 (1.6)	393.5 ⁹⁴
	O	$1b_2$	520.3 (-0.1)	521.4 (1.0)	521.4 (1.0)	521.4 (1.0)	520.4 ⁹⁵
H_2O	O	$3a_1$	524.4 (-0.7)	525.5 (0.4)	525.5 (0.4)	525.5 (0.4)	525.1 ⁹⁵
	O	$1b_1$	526.7 (-0.1)	527.8 (1.0)	527.8 (1.0)	527.7 (0.9)	526.8 ⁹⁵
	С	2a''	281.2 (0.0)	281.8 (0.6)	281.7 (0.5)	281.6 (0.4)	281.2 ⁹⁶
	С	7a'	279.4 (0.0)	280.0 (0.6)	279.9 (0.5)	279.8 (0.4)	279.4^{96}
CH₃OH	С	6a'	277.1(-0.3)	277.6 (0.2)	277.5 (0.1)	277.4 (0.0)	277.4^{96}
C113O11	O	2a''	527.1 (-0.7)	528.4 (0.6)	528.2 (0.4)	528.0 (0.2)	527.8^{96}
	O	7a'	525.3 (-0.9)	526.6 (0.4)	526.4 (0.2)	526.2 (0.0)	526.2 ⁹⁶
	O	6a'	522.9 (-0.9)	524.3 (0.5)	524.0 (0.2)	523.8 (0.0)	523.8 ⁹⁶
CH_4	C	$1t_2$	276.2 (-0.1)	276.6 (0.3)	276.7 (0.4)	276.7 (0.4)	276.3 ⁹⁷
	C	$1\pi_u$	280.9 (1.4)	279.2 (-0.4)	279.7 (0.2)	280.3 (0.7)	279.6 ⁹⁸
	С	$3\sigma_u$	280.6 (1.1)	278.9 (-0.7)	279.4 (-0.1)	280.0(0.4)	279.6^{98}
CO_2	O	$1\pi_g$	526.8 (-1.5)	528.9 (0.6)	528.1 (-0.2)	527.3 (-1.0)	528.3 ⁹⁸
	O	$1\pi_u$	522.7 (-1.7)	524.7 (0.3)	524.0 (-0.4)	523.2 (-1.2)	524.4 ⁹⁸
	O	$3\sigma_u$	522.4 (-2.0)	524.5 (0.1)	523.7 (-0.7)	522.9 (-1.5)	524.4 ⁹⁸
NH ₃	N	$3a_1$	394.4 (-0.7)	395.1 (0.1)	395.1 (0.1)	395.2 (0.1)	395.1 ⁹⁹
-11-13	N	1 <i>e</i>	388.6 (-0.2)	389.4 (0.6)	389.4 (0.6)	389.5 (0.7)	388.8 ⁹⁹
Ne	Ne	2 <i>p</i>	848.5 (0.0)	849.9 (1.4)	849.8 (1.3)	849.8 (1.3)	848.5 ¹⁰⁰
	NN	2π	394.4 (-1.2)	395.8 (0.2)	395.7 (0.1)	395.6 (0.0)	395.6 ⁹⁹
N_2O	NO	1π	391.9 (-2.9)	394.8 (0.0)	394.4 (-0.4)	393.9 (-0.9)	394.8 ⁹⁹
	NN	7σ	390.6 (-1.7)	392.0 (-0.3)	391.9 (-0.4)	391.8 (-0.5)	392.399
	NN	1π	388.6 (-2.0)	390.0 (-0.6)	389.9 (-0.7)	389.8 (-0.8)	390.699
	O	2π	527.0 (-1.8)	529.4 (0.6)	529.1 (0.3)	528.7 (-0.1)	528.899
	O	1π	521.1 (-2.8)	523.6 (-0.3)	523.3 (-0.6)	522.9 (-1.0)	523.999
	O	7σ	523.1 (-1.8)	525.6 (0.7)	525.3 (0.4)	524.9 (0.0)	524.9 ¹⁰¹
	0	6σ	519.8 (-1.3)	522.3 (1.1)	522.0 (0.8)	521.6 (0.4)	521.2 ¹⁰¹
	NO	7σ	393.9 (-2.2)	396.8 (0.7)	396.4 (0.3)	395.9 (-0.2)	396.1 ¹⁰¹
	NO	6σ	390.6 (-1.8)	393.5 (1.2)	393.1 (0.7)	392.7 (0.3)	392.4 ¹⁰¹
	NN	6σ	387.3 (-1.2)	388.7 (0.2)	388.6 (0.1)	388.5 (0.0)	388.5 ¹⁰¹
C_2H_4	C	$1b_{3u}$	279.7 (-0.2)	280.4 (0.5)	280.1 (0.2)	279.7 (-0.2)	279.9 ¹⁰²
	C	$1b_{3g}$	277.2 (-0.5)	277.9 (0.2)	277.6 (-0.1)	277.3 (-0.4)	277.7 ¹⁰²
	C	$3a_g$	275.4 (-0.4)	276.1 (0.3)	275.7 (-0.1)	275.4 (-0.4)	275.8 ¹⁰²
	C C	$1b_{2u} \ 2b_{1u}$	274.1 (-0.4) 270.7 (-0.6)	274.8 (0.3) 271.5 (0.2)	274.5 (0.0) 271.1 (-0.2)	274.2 (-0.3) 270.8 (-0.5)	274.5 ¹⁰² 271.3 ¹⁰²
PS _{min}	0.84	MAE	1.0	0.6	0.5	0.5	
PS _{min} PS _{ave}	0.84	RMSE	1.3	0.7	0.6	0.6	
1 Jave	0.70	MVIOL	1.5	0.7	0.0	0.0	

TABLE II. Vertical C–F K-edge emission energies \mathcal{E}_X computed with projected ΔMPn and EPT [P3+].

F $1a_2$ 678.3 (0.2) 678.2 (0.0) 677.8 (-0.3) 677.5 (-0.6)	Exp.
$ \begin{array}{c} {\rm CE} \\ {\rm CE} \\ {\rm CE} \\ {\rm CC} \\ {\rm CE} \\ {\rm CC} \\ {\rm CE} \\ {\rm CC} \\ {\rm CE} \\ {\rm C$	261.8 ¹⁰³
$ \begin{array}{c} \mathrm{CF_4} & \mathrm{C} & 4a_1 & 277.1 (0.1) & 277.2 (0.2) & 277.2 (0.2) & 277.2 (0.2) \\ \mathrm{F} & 1e & 676.4 (-0.2) & 676.1 (-0.5) & 675.9 (-0.7) & 675.7 (-0.9) \\ \mathrm{F} & 4t_2 & 677.3 (-0.3) & 677.0 (-0.6) & 676.8 (-0.8) & 676.6 (-1.0) \\ \mathrm{F} & 1t_1 & 678.5 (-0.3) & 678.2 (-0.6) & 678.0 (-0.8) & 677.8 (-1.0) \\ \mathrm{F} & 1t_1 & 678.5 (-0.3) & 678.2 (-0.6) & 676.1 (0.5) & 675.9 (0.3) \\ \mathrm{F} & 5a_1 & 674.4 (-1.1) & 676.2 (0.6) & 676.1 (0.5) & 675.9 (0.3) \\ \mathrm{F} & 5a_1 & 674.4 (-1.2) & 676.0 (0.4) & 675.9 (0.3) & 675.8 (0.2) \\ \mathrm{F} & 2e & 678.1 (-0.5) & 679.7 (1.1) & 679.6 (1.0) & 679.5 (0.9) \\ \mathrm{C} & 1e & 276.5 (0.3) & 276.9 (0.7) & 276.9 (0.7) & 276.9 (0.7) \\ \mathrm{C} & 5a_1 & 276.3 (0.1) & 276.7 (0.5) & 276.7 (0.5) & 276.8 (0.6) \\ \mathrm{C} & 2e & 280.1 (0.1) & 280.4 (0.4) & 280.5 (0.5) & 280.5 (0.5) \\ \mathrm{C} & 4a_1 & 269.5 (-0.5) & 269.9 (-0.1) & 269.9 (-0.1) \\ \mathrm{F} & 4a_1 & 668.4 (-1.0) & 668.4 (-1.0) & 668.1 (-1.3) & 667.9 (-1.5) \\ \mathrm{F} & 1b_2 & 673.5 (-0.9) & 673.6 (-0.8) & 673.3 (-1.1) & 673.0 (-1.4) \\ \mathrm{F} & 5a_1 & 673.7 (-0.7) & 673.4 (-0.7) & 673.4 (-1.0) & 673.2 (-1.2) \\ \mathrm{F} & 3b_1 & 673.8 (-0.6) & 673.9 (-0.5) & 673.6 (-0.8) & 673.3 (-1.1) \\ \mathrm{F} & 4a_1 & 667.7 (-0.4) & 677.1 (-0.3) & 676.8 (-0.6) & 676.5 (-0.9) \\ \mathrm{F} & 4b_1 & 677.7 (0.3) & 677.8 (0.4) & 677.5 (0.1) & 677.2 (-0.2) \\ \mathrm{F} & 6a_1 & 677.3 (-0.1) & 677.4 (0.0) & 677.1 (-0.3) & 676.8 (-0.6) \\ \mathrm{C} & 5a_1 & 277.3 (0.2) & 277.6 (0.5) & 277.6 (0.5) & 277.6 (0.5) \\ \mathrm{C} & 4a_1 & 272.0 (0.0) & 272.3 (0.3) & 272.3 (0.3) & 272.3 (0.3) \\ \mathrm{C} & 4a_1 & 272.0 (0.0) & 272.3 (0.3) & 272.3 (0.3) & 272.3 (0.3) \\ \mathrm{C} & 4a_1 & 274.5 (0.3) & 274.7 (0.5) & 277.6 (0.5) & 277.6 (0.5) & 277.6 (0.5) \\ \mathrm{C} & 4a_1 & 274.5 (0.3) & 274.7 (0.5) & 277.6 (0.5) & 277.7 (0.6) \\ \mathrm{C} & 4a_1 & 274.5 (0.3) & 274.7 (0.5) & 281.5 (0.6) & 281.2 (0.6) & 281.2 (0.6) \\ \mathrm{C} & 4e & 282.2 (0.4) $	279.5^{103}
$\begin{array}{c ccccccccccccccccccccccccccccccccccc$	284.4^{103}
$\begin{array}{c ccccccccccccccccccccccccccccccccccc$	277.0^{97}
$\begin{array}{c ccccccccccccccccccccccccccccccccccc$	$676.6^{104,105}$
$\begin{array}{c ccccccccccccccccccccccccccccccccccc$	677.6 ^{104,105}
$ \begin{array}{c} F \\ F \\ F \\ CH_3F \\ \end{array} \begin{array}{c} F \\ F \\ CH_3F \\ \end{array} \begin{array}{c} F \\ CH_3F \\ $	678.8 ^{104,105}
$ \begin{array}{c} F \\ CH_{3}F \\ CH_{$	675.6 ⁹⁷
$ \begin{array}{c} \mathrm{CH_3F} \\ \mathrm{C} \\ \mathrm{C} \\ \mathrm{C} \\ \mathrm{C} \\ \mathrm{C} \\ \mathrm{C} \\ \mathrm{Ie} \\ \mathrm{C} \\ \mathrm{C} \\ \mathrm{C} \\ \mathrm{S} \\ \mathrm{C} \\ \mathrm{C} \\ \mathrm{Ie} \\ \mathrm{C} \\ \mathrm{C} \\ \mathrm{C} \\ \mathrm{S} \\ \mathrm{S} \\ \mathrm{C} \\ \mathrm{C} \\ \mathrm{S} \\ \mathrm{Ie} \\ \mathrm{C} \\ \mathrm{C} \\ \mathrm{S} \\ \mathrm{S} \\ \mathrm{S} \\ \mathrm{C} \\ \mathrm{C} \\ \mathrm{S} \\ \mathrm{S} \\ \mathrm{S} \\ \mathrm{C} \\ \mathrm{C} \\ \mathrm{C} \\ \mathrm{S} \\ \mathrm{S} \\ \mathrm{S} \\ \mathrm{S} \\ \mathrm{C} \\ \mathrm{C} \\ \mathrm{C} \\ \mathrm{S} \\ \mathrm{S} \\ \mathrm{S} \\ \mathrm{C} \\ \mathrm{C} \\ \mathrm{C} \\ \mathrm{S} \\ \mathrm{S} \\ \mathrm{S} \\ \mathrm{C} \\ \mathrm{C} \\ \mathrm{C} \\ \mathrm{S} \\ \mathrm{S} \\ \mathrm{S} \\ \mathrm{C} \\ \mathrm{C} \\ \mathrm{C} \\ \mathrm{S} \\ \mathrm{S} \\ \mathrm{S} \\ \mathrm{C} \\ \mathrm{C} \\ \mathrm{C} \\ \mathrm{S} \\ \mathrm{S} \\ \mathrm{S} \\ \mathrm{C} \\ \mathrm{C} \\ \mathrm{C} \\ \mathrm{S} \\ \mathrm{S} \\ \mathrm{S} \\ \mathrm{C} \\ \mathrm{C} \\ \mathrm{C} \\ \mathrm{S} \\ \mathrm{S} \\ \mathrm{C} \\ \mathrm{C} \\ \mathrm{C} \\ \mathrm{S} \\ \mathrm{S} \\ \mathrm{C} \\ \mathrm{C} \\ \mathrm{C} \\ \mathrm{S} \\ \mathrm{S} \\ \mathrm{C} \\ \mathrm{C} \\ \mathrm{C} \\ \mathrm{S} \\ \mathrm{S} \\ \mathrm{C} \\ \mathrm{C} \\ \mathrm{C} \\ \mathrm{C} \\ \mathrm{S} \\ \mathrm{S} \\ \mathrm{C} \\ \mathrm{C} \\ \mathrm{C} \\ \mathrm{C} \\ \mathrm{S} \\ \mathrm{S} \\ \mathrm{C} \\ \mathrm{C} \\ \mathrm{C} \\ \mathrm{C} \\ \mathrm{S} \\ \mathrm{S} \\ \mathrm{C} \\ \mathrm$	675.6 ⁹⁷
$\begin{array}{c} \text{C.T.S.F.} \\ \text{C.} \\ \text{C.} \\ \text{C.} \\ \text{Sa}_{1} \\ \text{C.76.3} & (0.1) \\ \text{C.} \\ \text{Sa}_{1} \\ \text{C.76.3} & (0.1) \\ \text{C.} \\ \text{C.} \\ \text{Sa}_{1} \\ \text{C.76.3} & (0.1) \\ \text{C.} \\ \text{C.} \\ \text{C.} \\ \text{Se} \\ \text{280.1} & (0.1) \\ \text{280.4} & (0.4) \\ \text{280.5} & (0.5) \\ \text{280.9} & (-0.1) \\ \text{280.9} & (-0.1) \\ \text{280.9} & (-0.1) \\ \text{269.9} & (-0.1) \\ \text{267.8} & (-0.8) \\ \text{373.3} & (-1.1) \\ \text{673.4} & (-1.0) \\ \text{673.3} & (-1.1) \\ \text{678.8} & (-0.8) \\ \text{677.5} & (-0.8) \\ 67$	678.6 ⁹⁷
$\begin{array}{c ccccccccccccccccccccccccccccccccccc$	669.0^{97}
$\begin{array}{c} C \\ C $	276.2^{103}
$\begin{array}{c} C \\ \\ \\ \\ \\ \\ \\ \\ \\ \\ \\ \\ \\ \\ \\ \\ \\ \\ $	276.2^{103}
$\begin{array}{c ccccccccccccccccccccccccccccccccccc$	280.0^{103}
$\begin{array}{cccccccccccccccccccccccccccccccccccc$	270.0^{103}
$\begin{array}{c ccccccccccccccccccccccccccccccccccc$	669.4 ⁹⁷
$\begin{array}{cccccccccccccccccccccccccccccccccccc$	674.4^{97}
$\begin{array}{c ccccccccccccccccccccccccccccccccccc$	674.4^{97}
$\begin{array}{c ccccccccccccccccccccccccccccccccccc$	674.4^{97}
$ \begin{array}{cccccccccccccccccccccccccccccccccccc$	677.4^{97}
$\begin{array}{c} F \\ CH_2F_2 \\ F \\ 2b_2 \\ CH_2F_2 \\ CH_2F_2 \\ F \\ 2b_2 \\ CH_2F_2 \\ CH_2F_2 \\ CH_2F_2 \\ F \\ 2b_2 \\ CH_2F_2 \\ CH_2$	677.4^{97}
$\begin{array}{cccccccccccccccccccccccccccccccccccc$	677.4^{97}
$\begin{array}{cccccccccccccccccccccccccccccccccccc$	680.0^{97}
$\begin{array}{cccccccccccccccccccccccccccccccccccc$	277.1^{103}
$\begin{array}{cccccccccccccccccccccccccccccccccccc$	277.1^{103}
$\begin{array}{cccccccccccccccccccccccccccccccccccc$	277.1^{103}
$\begin{array}{cccccccccccccccccccccccccccccccccccc$	272.0^{103}
$\begin{array}{cccccccccccccccccccccccccccccccccccc$	280.6^{103}
$\begin{array}{cccccccccccccccccccccccccccccccccccc$	280.6^{103}
$\begin{array}{cccccccccccccccccccccccccccccccccccc$	282.4^{103}
$\begin{array}{cccccccccccccccccccccccccccccccccccc$	274.2^{103}
$\begin{array}{cccccccccccccccccccccccccccccccccccc$	278.2^{103}
$\begin{array}{cccccccccccccccccccccccccccccccccccc$	278.2^{103}
$ \begin{array}{cccccccccccccccccccccccccccccccccccc$	281.8 ¹⁰³
CHF ₃ F $4a_1$ 668.9 (-1.1) 668.8 (-1.2) 668.5 (-1.5) 668.2 (-1.8) F $5a_1$ 672.6 (-1.0) 672.5 (-1.1) 672.2 (-1.4) 671.9 (-1.7) F $3e$ 673.2 (-0.4) 673.0 (-0.6) 672.7 (-0.9) 672.4 (-1.2) F $4e$ 676.6 (-0.1) 676.5 (-0.2) 676.2 (-0.5) 675.9 (-0.8) F $5e$ 677.7 (-0.5) 677.5 (-0.6) 677.2 (-0.9) 676.9 (-1.2) F $1a_2$ 678.3 (0.2) 678.2 (0.0) 677.8 (-0.3) 677.5 (-0.6)	284.3 ¹⁰³
F $5a_1$ 672.6 (-1.0) 672.5 (-1.1) 672.2 (-1.4) 671.9 (-1.7) F $3e$ 673.2 (-0.4) 673.0 (-0.6) 672.7 (-0.9) 672.4 (-1.2) F $4e$ 676.6 (-0.1) 676.5 (-0.2) 676.2 (-0.5) 675.9 (-0.8) F $5e$ 677.7 (-0.5) 677.5 (-0.6) 677.2 (-0.9) 676.9 (-1.2) F $1a_2$ 678.3 (0.2) 678.2 (0.0) 677.8 (-0.3) 677.5 (-0.6)	670.0 ⁹⁷
F $3e$ $673.2 (-0.4)$ $673.0 (-0.6)$ $672.7 (-0.9)$ $672.4 (-1.2)$ F $4e$ $676.6 (-0.1)$ $676.5 (-0.2)$ $676.2 (-0.5)$ $675.9 (-0.8)$ F $5e$ $677.7 (-0.5)$ $677.5 (-0.6)$ $677.2 (-0.9)$ $676.9 (-1.2)$ F $1a_2$ $678.3 (0.2)$ $678.2 (0.0)$ $677.8 (-0.3)$ $677.5 (-0.6)$	673.6 ⁹⁷
F 4e 676.6 (-0.1) 676.5 (-0.2) 676.2 (-0.5) 675.9 (-0.8) F 5e 677.7 (-0.5) 677.5 (-0.6) 677.2 (-0.9) 676.9 (-1.2) F 1a ₂ 678.3 (0.2) 678.2 (0.0) 677.8 (-0.3) 677.5 (-0.6)	673.6 ⁹⁷
F 5e 677.7 (-0.5) 677.5 (-0.6) 677.2 (-0.9) 676.9 (-1.2) F 1a ₂ 678.3 (0.2) 678.2 (0.0) 677.8 (-0.3) 677.5 (-0.6)	676.7 ⁹⁷
F $1a_2$ 678.3 (0.2) 678.2 (0.0) 677.8 (-0.3) 677.5 (-0.6)	678.1 ^{97,105,106}
F $1u_2$ 0/8.3 (0.2) 0/8.2 (0.0) 0/7.3 (-0.5) 0/7.3 (-0.0) F $6a_1$ 678.7 (0.6) 678.6 (0.5) 678.3 (0.2) 678.0 (-0.1)	678.1 ^{97,105,106}
1 001 070.7 (0.0) 070.0 (0.3) 070.3 (0.4) 070.0 (-0.1)	678.1 ^{97,105,106}
	680.8 ^{107,108}
	677.9 ^{107,108}
F ₂ F $1\pi_u$ 676.1 (-1.8) 678.7 (0.8) 678.3 (0.4) 677.8 (-0.1) F $3\sigma_g$ 673.7 (-1.9) 676.3 (0.7) 675.9 (0.3) 675.4 (-0.2)	677.9 675.6 107,108
PS _{min} 0.84 MAE 0.5 0.5 0.6 0.7	
PS _{ave} 0.91 RMSE 0.7 0.6 0.7 0.8	

TABLE III. Vertical C–N–O K-edge excitation energies ω_X computed with projected Δ MPn and EPT [P3+].

Molecule	Core	Orbital	$\Delta PUHF [P3+]$	$\Delta PUMP2 [P3+]$	ΔPUMP2.5 [P3+]	ΔPUMP3 [P3+]	Exp.
	С	2pπ*	285.8 (-1.6)	287.2 (-0.2)	287.1 (-0.3)	287.1 (-0.3)	287.4 ¹⁰⁹
	С	$3s\sigma$	291.6 (-0.8)	292.9 (0.6)	292.9 (0.5)	292.9 (0.5)	292.4^{109}
	С	$3p\pi$	292.6 (-0.7)	294.0 (0.7)	293.9 (0.6)	293.9 (0.6)	293.3^{109}
	С	$4s\sigma$	292.7 (-2.1)	294.0 (-0.8)	294.0 (-0.8)	293.9 (-0.9)	294.8^{110}
	С	$3d\sigma$	293.6 (-1.2)	295.0 (0.2)	295.0 (0.2)	294.9 (0.1)	294.8^{110}
	С	$4p\pi$	293.9 (-0.9)	295.2 (0.5)	295.2 (0.4)	295.2 (0.4)	294.8^{109}
	С	$5p\pi$	294.1 (-1.2)	295.5 (0.2)	295.5 (0.2)	295.4 (0.1)	295.3^{109}
	С	$3d\pi$	293.9 (-0.7)	295.3 (0.7)	295.2 (0.6)	295.2 (0.6)	294.6^{109}
CO	С	$6p\pi$	294.9 (-0.7)	296.3 (0.7)	296.3 (0.7)	296.2 (0.6)	295.6^{109}
	O	$2p\pi^*$	532.7 (-1.5)	534.3 (0.1)	534.1 (-0.1)	533.9 (-0.3)	534.2^{111}
	O	$3s\sigma$	537.6 (-1.4)	539.2 (0.3)	539.0 (0.1)	538.8 (-0.1)	538.9^{112}
	O	$4s\sigma$	538.7 (-2.1)	540.3 (-0.5)	540.1 (-0.7)	539.9 (-0.9)	540.8^{112}
	O	$3d\sigma$	539.6 (-1.4)	541.2 (0.2)	541.0 (0.0)	540.8 (-0.2)	541.0^{112}
	O	$3p\pi$	538.7 (-1.2)	540.3 (0.4)	540.1 (0.2)	539.9 (0.0)	539.9^{112}
	O	$4p\pi$	539.8 (-1.4)	541.5 (0.2)	541.3 (0.0)	541.1 (-0.2)	541.3112
	O	5 <i>p</i> π	540.2 (-1.6)	541.8 (0.0)	541.6 (-0.2)	541.4 (-0.4)	541.8^{112}
	O	6 <i>p</i> π	540.9 (-1.1)	542.5 (0.5)	542.3 (0.3)	542.1 (0.1)	542.0^{112}
	O	$3d\pi$	539.9 (-1.2)	541.5 (0.4)	541.3 (0.2)	541.1 (0.0)	541.0 ¹¹²
	N	$2p\pi_{g}$	399.7 (-1.3)	401.7 (0.7)	401.4 (0.4)	401.0 (0.0)	401.0^{113}
	N	$3s\sigma_g^s$	405.1 (-1.0)	407.2 (1.1)	406.8 (0.7)	406.5 (0.4)	406.1^{113}
N	N	$3p\pi_u$	406.1 (-0.9)	408.2 (1.2)	407.9 (0.9)	407.5 (0.5)	407.0^{113}
N_2	N	$3p\sigma_u$	406.2 (-1.1)	408.3 (1.0)	407.9 (0.6)	407.6 (0.3)	407.3113
	N	$3d\sigma_g$	407.2 (-0.8)	409.3 (1.3)	408.9 (0.9)	408.6 (0.6)	408.0^{113}
	N	$3d\pi_g$	407.4 (-0.9)	409.5 (1.2)	409.1 (0.8)	408.8 (0.5)	408.3 ¹¹³
NO ^a	N	$2p\pi^*$	398.1 (-1.6)	400.0 (0.3)	399.8 (0.1)	399.7 (0.0)	399.781
	N	3 <i>s</i> σ	405.5 (-1.1)	407.4 (0.8)	407.3 (0.7)	407.1 (0.5)	406.6^{114}
	N	$3p\sigma$	406.6 (-1.2)	408.5 (0.8)	408.3 (0.6)	408.2 (0.4)	407.8^{114}
	N	$3p\pi$	406.6 (-1.1)	408.5 (0.9)	408.4 (0.7)	408.2 (0.5)	407.7^{114}
	N	$4s\sigma$	408.0 (-0.5)	410.0 (1.5)	409.8 (1.3)	409.6 (1.1)	408.5^{114}
	N	$3d\pi$	407.8 (-0.9)	409.8 (1.0)	409.6 (0.9)	409.5 (0.7)	408.8^{114}
	N	$4p\pi$	408.2 (-0.8)	410.1 (1.2)	410.0 (1.0)	409.8 (0.9)	408.9^{114}
H_2O	O	$3sa_1$	532.9 (-1.1)	533.9 (-0.1)	533.9 (-0.1)	533.9 (-0.1)	534.0 ¹¹⁵
	O	$3pb_2$	535.1 (-0.8)	536.2 (0.3)	536.2 (0.3)	536.2 (0.3)	535.9 ¹¹⁵
	O	$3pa_1$	536.3 (-0.8)	537.4 (0.3)	537.4 (0.3)	537.4 (0.3)	537.1 ¹¹⁵
	Ō	$3pb_1$	536.2 (-0.9)	537.3 (0.2)	537.3 (0.2)	537.3 (0.2)	537.1 ¹¹⁵
CH ₄	С	$3sa_1$	285.8 (-1.2)	286.2 (-0.8)	286.3 (-0.8)	286.3 (-0.7)	287.0 ¹¹⁶
	С	$3pt_2$	287.7 (-0.7)	288.1 (-0.3)	288.2 (-0.2)	288.2 (-0.2)	288.4^{116}
	С	$4pt_2^2$	288.6 (-1.1)	289.0 (-0.7)	289.1 (-0.6)	289.1 (-0.5)	289.7116
	C	$4sa_1$	288.7 (-0.4)	289.1 (0.0)	289.2 (0.1)	289.3 (0.1)	289.1116
	Č	$5pt_2$	289.3 (-0.7)	289.7 (-0.3)	289.7 (-0.3)	289.8 (-0.2)	290.0^{116}
	C	$6pt_2$	290.2 (-0.1)	290.6 (0.3)	290.7 (0.3)	290.8 (0.4)	290.4^{116}
NH_3	N	$3sa_1$	399.6 (-1.0)	400.3 (-0.3)	400.4 (-0.3)	400.4 (-0.2)	400.7^{116}
	N	3ре	401.8 (-0.5)	402.6 (0.2)	402.6 (0.3)	402.7 (0.3)	402.3116
	N	$3pa_1$	402.4 (-0.4)	403.2 (0.3)	403.2 (0.4)	403.3 (0.4)	402.9^{116}
	N	$4sa_1$	403.2 (-0.4)	403.9 (0.3)	403.9 (0.4)	404.0 (0.4)	403.6^{116}
	N	4 <i>pe</i>	403.2 (-0.9)	403.9 (-0.2)	404.0 (-0.2)	404.0 (-0.1)	404.2^{116}
	N	5 <i>pe</i>	403.7 (-0.9)	404.4 (-0.2)	404.5 (-0.1)	404.5 (-0.1)	404.6 ¹¹⁵

TABLE III. (Continued.)

Molecule	Core	Orbital	$\Delta PUHF [P3+]$	$\Delta PUMP2 [P3+]$	Δ PUMP2.5 [P3+]	$\Delta PUMP3 [P3+]$	Exp.
	NN	2pπ*	399.8 (-1.2)	401.2 (0.2)	401.1 (0.1)	401.1 (0.1)	401.0117
	NN	$3s\sigma$	402.4 (-1.5)	403.8 (0.0)	403.7 (-0.1)	403.6 (-0.2)	403.8^{117}
	NO	$2p\pi$	402.4 (-2.2)	405.3 (0.7)	404.9 (0.3)	404.4 (-0.2)	404.6^{117}
	NN	$3p\pi$	404.9 (-0.9)	406.3 (0.6)	406.3 (0.5)	406.2 (0.4)	405.8^{117}
	NN	$4s\sigma$	405.2 (-1.1)	406.6(0.4)	406.5 (0.3)	406.4 (0.2)	406.2^{117}
	NN	$3d\pi$	406.3 (-0.7)	407.7 (0.8)	407.6 (0.7)	407.5 (0.6)	406.9^{117}
N_2O	NN	$4p\pi$	406.1 (-1.0)	407.5 (0.4)	407.4 (0.3)	407.3 (0.2)	407.1^{117}
	NN	$3d\sigma$	405.3 (-1.9)	406.7 (-0.5)	406.6 (-0.6)	406.5 (-0.7)	407.2^{117}
	NO	$3s\sigma$	406.5 (-0.9)	409.5 (2.0)	409.0 (1.5)	408.6 (1.1)	407.5^{117}
	O	$2p\pi^*$	533.6 (-1.0)	536.1 (1.5)	535.8 (1.2)	535.4 (0.8)	534.6^{117}
	O	$3s\sigma$	534.7 (-1.9)	537.2 (0.6)	536.8 (0.2)	536.5 (-0.1)	536.6^{117}
	O	$3p\pi$	537.5 (-1.3)	540.0 (1.2)	539.7 (0.9)	539.3 (0.5)	538.8 ¹¹⁷
	O	$4s\sigma$	537.7 (-1.4)	540.2 (1.1)	539.8 (0.7)	539.5 (0.4)	539.1 ^{117,11}
	O	σ^*	531.5 (-1.5)	533.0 (0.0)	532.8 (-0.2)	532.6 (-0.4)	533.0119
	O	σ^*	534.8 (-0.5)	536.3 (1.0)	536.1 (0.8)	535.9 (0.6)	535.3 ¹¹⁹
H_2O_2	O	σ^*	536.1 (0.8)	537.6 (2.3)	537.3 (2.0)	537.1 (1.8)	535.3 ¹¹⁹
	O	3 <i>s</i>	537.2 (0.4)	538.7 (1.9)	538.4 (1.6)	538.2 (1.4)	536.8119
	O	3 <i>p</i>	537.2 (-1.1)	538.7 (0.4)	538.4 (0.1)	538.2 (-0.1)	538.3 ¹¹⁹
C_2H_4	C	π^*	283.9 (-0.7)	284.6 (0.0)	284.3 (-0.4)	284.0 (-0.7)	284.7^{109}
	C	3 <i>s</i>	286.6 (-0.7)	287.3 (0.1)	287.0 (-0.3)	286.6 (-0.6)	287.2^{109}
	C	3 <i>p</i>	287.4(-0.5)	288.1 (0.2)	287.8 (-0.1)	287.4(-0.4)	287.9^{109}
	C	4p	288.8 (-0.6)	289.5 (0.1)	289.1 (-0.3)	288.8 (-0.6)	289.4^{109}
	C	5 <i>p</i>	288.9 (-1.0)	289.6 (-0.3)	289.3 (-0.6)	289.0 (-1.0)	289.9^{109}
PS _{min}	0.89	MAE	1.0	0.6	0.5	0.4	
PS _{ave}	0.98	RMSE	1.1	0.8	0.6	0.5	

 $a^{2}\Delta - {}^{3}\Pi$ channel.

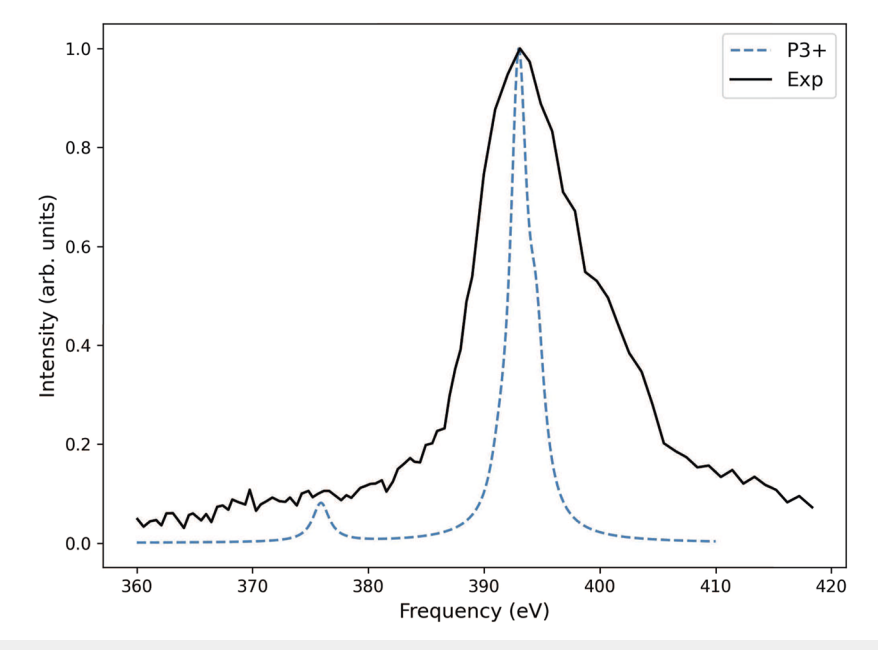


FIG. 3. Simulated emission spectra for N_2 . IP $_{\text{core}}$ computed with $\Delta PUMP3$. EPT results and relative intensities obtained with an HF/cc-pVTZ reference. Experimental spectrum 120 reprinted with permission from R. E. LaVilla, J. Chem. Phys. 56, 2345–2349 (1972). Copyright 1972 AIP Publishing LLC.

There are a few important caveats to the types of excited states accessible with single-reference methods. We again turn to the NO example. The $1s\to 2p\pi^*$ excitation leads to multiple electronic states: $^4\Sigma^-$, $^2\Sigma^-$, $^2\Delta$, and $^2\Sigma^+$. The high-spin quartet $^4\Sigma^-$ and a $^2\Delta$ state in the core open-shell, valence-paired configuration can be approximated by a single Slater determinant. However, the $^2\Sigma^-$ and $^2\Sigma^+$ doublet states with three unpaired spins in 1s and $2p\pi^*$ orbitals must be spin-adapted. States that require the recoupling of spin angular momenta and recovery of opposite-spin correlation effects are not directly accessible with single determinant SCF. Determination of excited electronic spin states will require information contained in multi-configurational wavefunctions.

In addition, this study only examines vertical transitions from ground state geometries. Molecular x-ray spectra may exhibit fine vibrational structure for core excitations or Jahn-Teller splitting following core-ionization. Furthermore, the two-state Δ -based methods employed here are quantitatively valid only for transitions involving one electron or one particle-hole pair. These approaches are not immediately applicable for describing two-electron processes inherent in resonant inelastic x-ray scattering (RIXS) and Auger spectra. For coherent processes in molecules with equivalent atoms, the convenient option of core-hole localization is no longer viable since decay into specific delocalized core orbitals is necessary to guarantee proper final-state symmetries and spectral patterns.⁶⁹ Koopmans-like interpretations fail to describe shake processes and satellite structure in the instance of strong configuration interaction (CI) and large ORX. Diagonal quasiparticle methods with uncorrelated HF orbitals fall short in this category, and thus, non-diagonal self-energy approximations are typically applied.^{70–72} To capture the important many-body effects, response theories can be tailored to model x-ray transitions involving two electrons. 11,73-79

The inadequacies of single-reference methods are also pronounced in molecules with multi-reference open-shell character. For example, multi-configurational $\Delta SCF\ IP_{core}$ estimates 80 of the $^4\Sigma^-$ and $^2\Sigma^-$ states of O_2^+ with orbital optimization, Slater-type basis sets, and core-localization still deviate $\sim\!1\!-\!2$ eV from the experiment. Improved accuracy is not expected from projected energies beginning with one HF determinant, especially considering the non-variational nature of the chosen PAV method. Thus, the limits of mean-field methods become apparent when electron correlation is strong. Very accurate vertical IPs for open-shell or strongly correlated molecules, such as O_2 , can be realized with spin-adapted multiconfigurational propagator methods 82,83 and alternative choices of the reference wavefunction. 84

Some demonstrative examples for simulating non-resonant XES are shown in Figs. 3–5. Peak positions and relative intensities for main-line transitions are adequately reproduced with P3+ and population analysis of the ground state MOs. In the theoretical spectra for N_2 , the low PS (0.608) for the $2\sigma_g$ orbital leads to a shift in the low intensity peak towards the main peak by about 3 eV. This result is not atypical for inner-valence IPs where considerable relaxation effects are present and better accounted for in higher order self-energy approximations. For all other transitions depicted in the calculated XES spectra of N_2 , C_2H_4 , and H_2O , the canonical Hartree–Fock orbitals are sufficient representations of the Dyson orbitals (PS > 0.85) with the selected diagonal method. Characterization of satellite structure necessitates a more detailed analysis with non-diagonal self-energy approximations or CI methods. 71,85

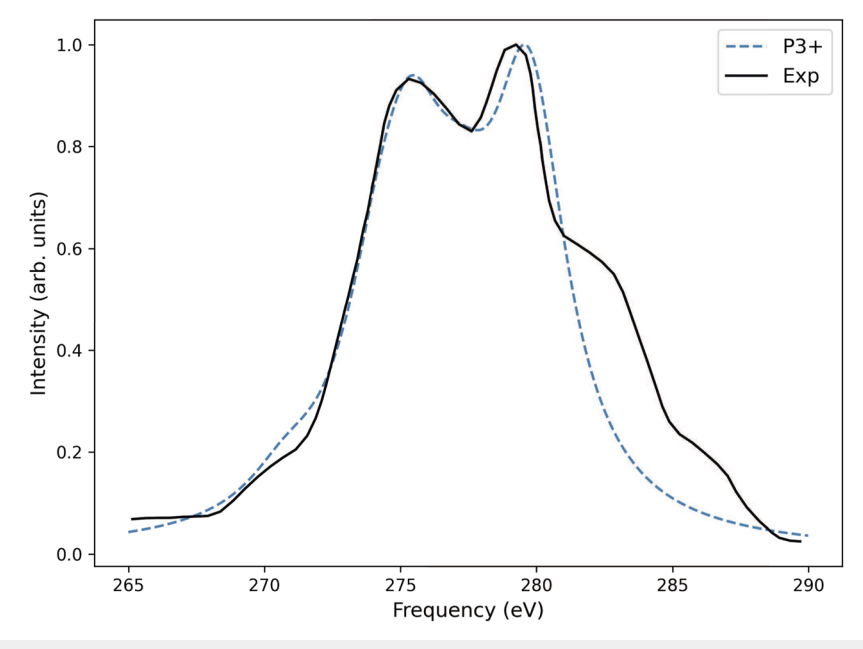


FIG. 4. Simulated emission spectra for C₂H₄. IP_{core} computed with ΔPUMP3. EPT results obtained with a HF/cc-pVTZ reference. Relative intensities are obtained with an extended Hückel reference. Experimental spectrum reprinted with permission from R. Manne, J. Chem. Phys. **52**, 5733–5739 (1970). Copyright 1970 AIP Publishing LLC.

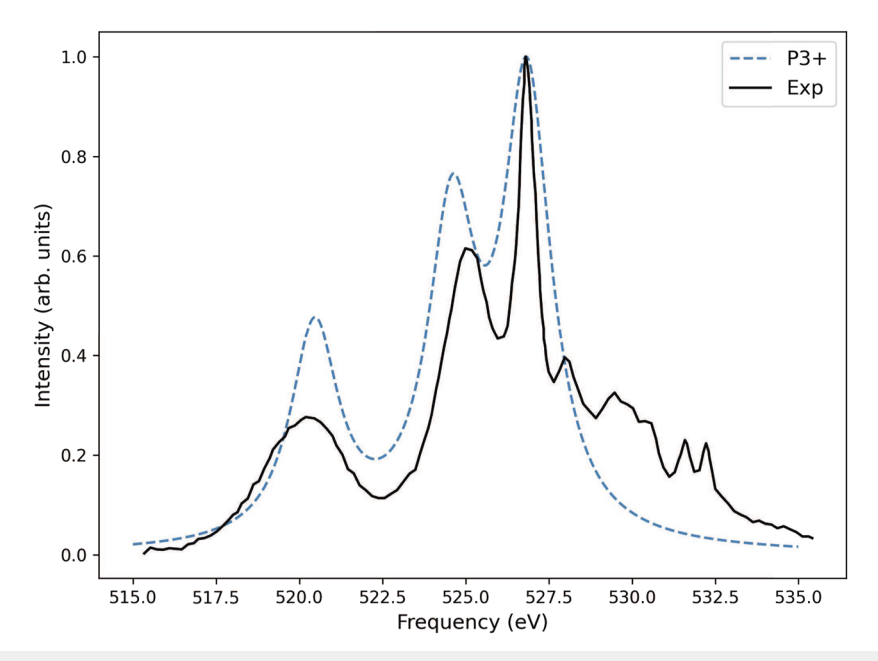


FIG. 5. Simulated emission spectra for H₂O. IP_{core} computed with ΔPUMP3. EPT results and relative intensities obtained with a HF/cc-pVTZ reference. An alignment shift of -0.9 eV is applied to the simulated spectra. Experimental spectrum reprinted with permission from J.-E. Rubensson et al., J. Chem. Phys. 82, 4486-4491 (1985). Copyright 1985 AIP Publishing LLC.

Oscillator strengths for x-ray absorption, particularly for Rydberg transitions, can be evaluated through quantum defect analysis with EPT or Δ SCF for reconstructing spectra. ^{86–88} intensities for N-conserving excitations may be calculated directly with projected dipole moments between the orbital-optimized ground state and core-excited state wavefunctions. The scope of these methodologies warrants a separate study.

The overall results presented here highlight the accuracy of Δ -based models using HF, MP, and EPT for computing K-shell excitation and non-resonant emission energies of molecules containing second-row p-block elements. The single-reference models used here are deemed appropriate within the one-electron portrait of X-ray transitions. Composite methods, like those featured in this work, are advantageous since they are modular and allow for specific observable quantities to be approximated independently at the desired levels of theory. Extensions of composite models to treat two-electron processes and simulate satellite structure can be made possible with two-electron Green's functions and non-diagonal selfenergy approximations. Finally, the inclusion of accurate relativistic effects is of greater importance to the overall spectral profile and shift in IP_{core} with increasing Z. For describing inner-shell transitions in heavier elements, the use of relativistic Hamiltonians is preferred over atom-specific ad hoc corrections based on two-electron ions or semi-empirical fits used here.

IV. CONCLUSIONS

We have examined Δ -based composite models for computing *K*-edge emission and excitation energies. The models' construction and performance are comparable to modern STEX methods and a practical approach for estimating core-level energetics for oneelectron processes is established. The models employed here appear to be competitive with ADC, EOM-CCSD, and TD-DFT for oneparticle transitions. Notwithstanding the additive propagation of errors and reliance on the cancellation of such errors in Δ -based approaches, the combination of projected SCF, MP, and propagator theories afford accurate results with reasonable computational

SUPPLEMENTARY MATERIAL

See the supplementary material for computed intermediate data for presented results.

ACKNOWLEDGMENTS

This research was supported by the National Science Foundation (Grant No. CHE-1848580).

AUTHOR DECLARATIONS

Conflict of Interest

The authors have no conflicts to disclose.

Author Contributions

Abdulrahman Y. Zamani: Conceptualization (lead); Data curation (lead); Methodology (lead); Writing - original draft (lead); Writing review & editing (equal). Hrant P. Hratchian: Funding acquisition (lead); Project administration (equal); Resources (lead); Writing review & editing (equal).

DATA AVAILABILITY

The data that support the findings of this study are available from the corresponding author upon reasonable request.

REFERENCES

- ¹ Synchrotron Radiation in Materials Science, edited by C. Fan and Z. Zhao (Wiley,
- ²X. Liu, W. Yang, and Z. Liu, "Recent progress on synchrotron-based in-situ soft X-ray spectroscopy for energy materials," Adv. Mater. 26, 7710-7729 (2014).
- ³F. Lin, Y. Liu, X. Yu, L. Cheng, A. Singer, O. G. Shpyrko, H. L. Xin, N. Tamura, C. Tian, T.-C. Weng, X.-Q. Yang, Y. S. Meng, D. Nordlund, W. Yang, and M. M. Doeff, "Synchrotron X-ray analytical techniques for studying materials electrochemistry in rechargeable batteries," Chem. Rev. 117, 13123-13186 (2017). ⁴P. M. Kraus, M. Zürch, S. K. Cushing, D. M. Neumark, and S. R. Leone, "The ultrafast X-ray spectroscopic revolution in chemical dynamics," Nat. Rev. Chem **2**, 82–94 (2018).
- ⁵L. X. Chen, X. Zhang, and M. L. Shelby, "Recent advances on ultrafast X-ray spectroscopy in the chemical sciences," Chem. Sci. 5, 4136-4152 (2014).
- ⁶C. Bressler and M. Chergui, "Molecular structural dynamics probed by ultrafast X-ray absorption spectroscopy," Annu. Rev. Phys. Chem. 61, 263-282 (2010).
- ⁷C. Bressler and M. Chergui, "Ultrafast X-ray absorption spectroscopy," ChemInform 35, 1781-1812 (2004).
- $^{\mathbf{8}}\text{P. S.}$ Bagus, "Self-consistent-field wave functions for hole states of some Ne-like and Ar-like ions," Phys. Rev. 139, A619-A634 (1965).
- ⁹P. S. Bagus and H. F. Schaefer III, "Direct near-Hartree–Fock calculations on the 1s hole states of NO⁺," J. Chem. Phys. 55, 1474–1475 (1971).
- ¹⁰C. Liegener and H. Ågren, "Electronic spectra of finite polyenes and polyacetylene obtained by electron and polarization propagator calculations," Theor. Chim. Acta 89, 335-362 (1994).
- ¹¹K. D. Nanda and A. I. Krylov, "A simple molecular orbital picture of RIXS distilled from many-body damped response theory," J. Chem. Phys. 152, 244118
- $^{\bf 12}$ J. D. Wadey and N. A. Besley, "Quantum chemical calculations of x-ray emission spectroscopy," J. Chem. Theory Comput. 10, 4557-4564 (2014).
- 13T. Fransson and A. Dreuw, "Simulating X-ray emission spectroscopy with algebraic diagrammatic construction schemes for the polarization propagator," Chem. Theory Comput. 15, 546-556 (2019).
- ¹⁴K. Ohno and T. Aoki, "Extended quasiparticle approach to non-resonant and resonant X-ray emission spectroscopy," Phys. Chem. Chem. Phys. 24, 16586-16595 (2022).
- ¹⁵H. Ågren, V. Carravetta, O. Vahtras, and L. G. Pettersson, "Direct, atomic orbital, static exchange calculations of photoabsorption spectra of large molecules and clusters," Chem. Phys. Lett. 222, 75-81 (1994).
- ¹⁶H. Ågren, V. Carravetta, O. Vahtras, and L. G. M. Pettersson, "Direct SCF direct static-exchange calculations of electronic spectra," Theor. Chem. Acc. 97, 14-40 (1997).
- ¹⁷C. A. Marante, L. Greenman, C. S. Trevisan, T. N. Rescigno, C. W. McCurdy, and R. R. Lucchese, "Validity of the static-exchange approximation for inner-shell photoionization of polyatomic molecules," Phys. Rev. A 102, 012815 (2020).
- ¹⁸K. Carter-Fenk, L. A. Cunha, J. E. Arias-Martinez, and M. Head-Gordon, "Electron-affinity time-dependent density functional theory: Formalism and applications to core-excited states," J. Phys. Chem. Lett. 13, 9664–9672 (2022).

 19 M. Nooijen and R. J. Bartlett, "Equation of motion coupled cluster method for
- electron attachment," J. Chem. Phys. 102, 3629-3647 (1995).

- ²⁰M. Nooijen and R. J. Bartlett, "Description of core-excitation spectra by the open-shell electron-attachment equation-of-motion coupled cluster method," . Chem. Phys. 102, 6735-6756 (1995).
- $^{\mathbf{21}}\mathrm{X}.$ Zheng and L. Cheng, "Performance of delta-coupled-cluster methods for calculations of core-ionization energies of first-row elements," J. Chem. Theory Comput. 15, 4945-4955 (2019).
- ²²M. Simons and D. A. Matthews, "Accurate core-excited states via inclusion of core triple excitations in similarity-transformed equation-of-motion theory," Chem. Theory Comput. 18, 3759-3765 (2022).
- ²³D. A. Matthews, "EOM-CC methods with approximate triple excitations applied to core excitation and ionisation energies," Mol. Phys. 118, e1771448
- ²⁴B. Pickup and O. Goscinski, "Direct calculation of ionization energies," Mol. Phys. 26, 1013-1035 (1973).
- ²⁵L. C. Snyder, "Core-electron binding energies and Slater atomic shielding constants," J. Chem. Phys. 55, 95-99 (1971).
- ²⁶L. S. Cederbaum and W. Domcke, "Localized and delocalized core holes and their interrelation," J. Chem. Phys. 66, 5084-5086 (1977).
- ²⁷N. A. Besley, A. T. B. Gilbert, and P. M. W. Gill, "Self-consistent-field calculations of core excited states," J. Chem. Phys. 130, 124308 (2009).
- ²⁸D. Danovich, "Green's function methods for calculating ionization potentials, electron affinities, and excitation energies," WIREs Comput. Mol. Sci. 1, 377-387
- ²⁹H. H. Corzo and J. V. Ortiz, "Electron propagator theory: Foundations and predictions," Adv. Quantum Chem. 74, 267–298 (2017).

 30 L. S. Cederbaum and W. Domcke, "Theoretical aspects of ionization poten-
- tials and photoelectron spectroscopy: A Green's function approach," Advances in Chemical Physics (John Wiley & Sons, 1977), Vol. 36, pp. 205-344.
- ³¹M. Nooijen and J. G. Snijders, "Coupled cluster Green's function method: Working equations and applications," Int. J. Quantum Chem. 48, 15-48 (1993).
- ³²A. T. B. Gilbert, N. A. Besley, and P. M. W. Gill, "Self-consistent field calculations of excited states using the maximum overlap method (MOM)," J. Phys. Chem. A 112, 13164-13171 (2008).
- 33 K. Carter-Fenk and J. M. Herbert, "State-targeted energy projection: A simple and robust approach to orbital relaxation of non-Aufbau self-consistent field solutions," J. Chem. Theory Comput. 16, 5067-5082 (2020).
- ³⁴H. H. Corzo, A. Abou Taka, A. Pribram-Jones, and H. P. Hratchian, "Using projection operators with maximum overlap methods to simplify challenging selfconsistent field optimization," J. Comput. Chem. 43, 382-390 (2022).
- 35 A. Dreuw and T. Fransson, "Using core-hole reference states for calculating X-ray photoelectron and emission spectra," Phys. Chem. Chem. Phys. 24, 11259-11267 (2022).
- ³⁶P.-O. Löwdin, "Quantum theory of many-particle systems. III. Extension of the Hartree-Fock scheme to include degenerate systems and correlation effects," Phys. Rev. 97, 1509-1520 (1955).
- ³⁷P.-O. Löwdin, "Expansion theorems for the total wave function and extended Hartree-Fock schemes," Rev. Mod. Phys. 32, 328-334 (1960).
- ³⁸H. B. Schlegel, "Møller-Plesset perturbation theory with spin projection," J. Phys. Chem. 92, 3075-3078 (1988).
- ³⁹ H. B. Schlegel, "Spin contamination," in *Encyclopedia of Computational Chem*istry, edited by P. von Ragué Schleyer, N. L. Allinger, T. Clark, J. Gasteiger, P. A. Kollman, H. F. Schaefer, and P. R. Schreiner (John Wiley & Sons, Ltd., 1998), pp. 2665-2671.
- $^{\mathbf{40}}$ W. Chen and H. B. Schlegel, "Evaluation of S 2 for correlated wave functions and spin projection of unrestricted Møller-Plesset perturbation theory," J. Chem. Phys. 101, 5957-5968 (1994).
- ⁴¹J. V. Ortiz, "Electron propagator theory: An approach to prediction and interpretation in quantum chemistry," WIREs Comput. Mol. Sci. 3, 123-142
- ⁴²H. H. Corzo, A. Galano, O. Dolgounitcheva, V. G. Zakrzewski, and J. V. Ortiz, "NR2 and P3+: Accurate, efficient electron-propagator methods for calculating valence, vertical ionization energies of closed-shell molecules," J. Phys. Chem. A 119, 8813-8821 (2015).
- ⁴³E. Opoku, F. Pawłowski, and J. V. Ortiz, "A new generation of diagonal selfenergies for the calculation of electron removal energies," J. Chem. Phys. 155, 204107 (2021).

- ⁴⁴E. Opoku, F. Pawłowski, and J. V. Ortiz, "Electron propagator self-energies versus improved GW100 vertical ionization energies," J. Chem. Theory Comput. **18**, 4927–4944 (2022).
- ⁴⁵E. Opoku, F. Pawłowski, and J. V. Ortiz, "Electron propagator theory of vertical electron detachment energies of anions: Benchmarks and applications to nucleotides," J. Phys. Chem. A 127, 1085–1101 (2023).
- ⁴⁶J. V. Ortiz, "An efficient, renormalized self-energy for calculating the electron binding energies of closed-shell molecules and anions," Int. J. Quantum Chem. **105**, 803–808 (2005).
- ⁴⁷J. V. Ortiz, "Dyson-orbital concepts for description of electrons in molecules," J. Chem. Phys. 153, 070902 (2020).
- ⁴⁸ M. Díaz Tinoco, H. H. Corzo, F. Pawłowski, and J. V. Ortiz, "Do Dyson orbitals resemble canonical Hartree–Fock orbitals?," Mol. Phys. 117, 2275–2283 (2019).
- ⁴⁹B. Samal and V. K. Voora, "Modeling nonresonant X-ray emission of secondand third-period elements without core-hole reference states and empirical parameters," J. Chem. Theory Comput. 18, 7272–7285 (2022).
 ⁵⁰V. Vaz da Cruz, S. Eckert, and A. Föhlisch, "TD-DFT simulations of K-edge
- ⁵⁰ V. Vaz da Cruz, S. Eckert, and A. Föhlisch, "TD-DFT simulations of K-edge resonant inelastic X-ray scattering within the restricted subspace approximation," Phys. Chem. Chem. Phys. 23, 1835–1848 (2021).
- ⁵¹L. Triguero, L. G. M. Pettersson, and H. Ågren, "Calculations of X-ray emission spectra of molecules and surface adsorbates by means of density functional theory," J. Phys. Chem. A 102, 10599–10607 (1998).
- ⁵²R. Manne, "Molecular orbital interpretation of x-ray emission spectra: Simple hydrocarbons and carbon oxides," J. Chem. Phys. **52**, 5733–5739 (1970).
- ⁵³ H. Ågren and J. Nordgren, "Ab initio Hartree-Fock calculations of molecular X-ray intensities. Validity of one-center approximations," Theor. Chim. Acta 58, 111–119 (1981).
- ⁵⁴K. E. Edgecombe and R. J. Boyd, "Atomic orbital populations and atomic charges from self-consistent field molecular orbital wavefunctions," J. Chem. Soc., Faraday Trans. 2 83, 1307–1315 (1987).
- ⁵⁵D. P. Chong, "Density-functional calculation of core-electron binding energies of C, N, O, and F," J. Chem. Phys. **103**, 1842–1845 (1995).
- ⁵⁶C. L. Pekeris, "Ground state of two-electron atoms," Phys. Rev. **112**, 1649–1658 (1958)
- ⁵⁷C. W. Scherr and J. N. Silverman, "Perturbation analysis of two- to four-electron variational wave functions," J. Chem. Phys. **37**, 1154–1156 (1962).
- ⁵⁸ R. H. Myhre, T. J. A. Wolf, L. Cheng, S. Nandi, S. Coriani, M. Gühr, and H. Koch, "A theoretical and experimental benchmark study of core-excited states in nitrogen," J. Chem. Phys. **148**, 064106 (2018).
- ⁵⁹W. Schwarz and R. J. Buenker, "Use of the *Z*+1-core analogy model: Examples from the core-excitation spectra of CO₂ and N₂O," Chem. Phys. **13**, 153–160 (1976).
- ⁶⁰R. D. Johnson III, NIST computational chemistry comparison and benchmark. Database NIST standard reference database number 101. Release 21, 2020, https://cccbdb.nist.gov/ (last accessed on 5 May 2022).
- ⁶¹ D. S. Ranasinghe, J. T. Margraf, A. Perera, and R. J. Bartlett, "Vertical valence ionization potential benchmarks from equation-of-motion coupled cluster theory and QTP functionals," J. Chem. Phys. 150, 074108 (2019).
- ⁶² M. J. Frisch, G. W. Trucks, H. B. Schlegel, G. E. Scuseria, M. A. Robb, J. R. Cheeseman, V. B. G. Scalmani, G. A. Petersson, H. Nakatsuji, X. Li, A. V. Marenich, M. Caricato, J. Bloino, B. G. Janesko, J. Zheng, R. Gomperts, B. Mennucci, H. P. Hratchian, J. V. Ortiz, A. F. Izmaylov, J. L. Sonnenberg, D. Williams-Young, F. Ding, F. Lipparini, F. Egidi, J. Goings, B. Peng, A. Petrone, T. Henderson, D. Ranasinghe, V. G. Zakrzewski, J. Gao, N. Rega, G. Zheng, W. Liang, M. Hada, M. Ehara, K. Toyota, R. Fukuda, J. Hasegawa, M. Ishida, T. Nakajima, Y. Honda, O. Kitao, H. Nakai, T. Vreven, K. Throssell, J. A. Montgomery, Jr., J. E. Peralta, F. Ogliaro, M. J. Bearpark, J. J. Heyd, E. N. Brothers, K. N. Kudin, V. N. Staroverov, T. A. Keith, R. Kobayashi, J. Normand, K. Raghavachari, A. P. Rendell, J. C. Burant, S. S. Iyengar, J. Tomasi, M. Cossi, J. M. Millam, M. Klene, C. Adamo, R. Cammi, J. W. Ochterski, R. L. Martin, K. Morokuma, O. Farkas, J. B. Foresman, and D. J. Fox, GAUSSIAN development version Revision J.15, Gaussian Inc., Wallingford CT, 2022.
- ⁶³B. P. Pritchard, D. Altarawy, B. Didier, T. D. Gibson, and T. L. Windus, "New Basis Set Exchange: An open, up-to-date resource for the molecular sciences community." I. Chem. Inf. Model. **59**, 4814–4820 (2019).
- ⁶⁴ A. Rohatgi, Webplotdigitizer: Version 4.6, 2022.

- ⁶⁵ A. Velasco, C. Lavín, M. Díaz-Tinoco, and J. Ortiz, "CaH Rydberg series, oscillator strengths and photoionization cross sections from Molecular Quantum Defect and Dyson Orbital theories," J. Quant. Spectrosc. Radiat. Transfer 187, 161–166 (2017).
- ⁶⁶H. Corzo, A. Velasco, C. Lavín, and J. Ortiz, "MgH Rydberg series: Transition energies from electron propagator theory and oscillator strengths from the molecular quantum defect orbital method," J. Quant. Spectrosc. Radiat. Transfer **206**, 323–327 (2018).
- 67 G. C. King, F. H. Read, and M. Tronc, "Investigation of the energy and vibrational structure of the inner shell $(1s)^{-1}(\pi 2p)^1\Pi$ state of the nitrogen molecule by electron impact with high resolution," Chem. Phys. Lett. **52**, 50–54 (1977).
- ⁶⁸ E. Ridente, D. Hait, E. A. Haugen, A. D. Ross, D. M. Neumark, M. Head-Gordon, and S. R. Leone, "Femtosecond symmetry breaking and coherent relaxation of methane cations via x-ray spectroscopy," Science 380, 713–717 (2023).
- ⁶⁹ P. Skytt, J. Guo, N. Wassdahl, J. Nordgren, Y. Luo, and H. Ågren, "Probing symmetry breaking upon core excitation with resonant x-ray fluorescence," Phys. Rev. A 52, 3572–3576 (1995).
- ⁷⁰L. Cederbaum, J. Schirmer, W. Domcke, and W. v. Niessen, "Complete breakdown of the quasiparticle picture for inner valence electrons," J. Phys. B: At. Mol. Phys. 10, L549 (1977).
- ⁷¹ J. V. Ortiz, "A nondiagonal, renormalized extension of partial third-order quasi-particle theory: Comparisons for closed-shell ionization energies," J. Chem. Phys. 108, 1008–1014 (1998).
- ⁷²O. Dolgounitcheva, V. G. Zakrzewski, and J. V. Ortiz, "Electron-propagator calculations on the photoelectron spectrum of ethylene," J. Chem. Phys. 114, 130–135 (2001).
- ⁷³D. R. Rehn, A. Dreuw, and P. Norman, "Resonant inelastic X-ray scattering amplitudes and cross sections in the algebraic diagrammatic construction/intermediate state representation (ADC/ISR) approach," J. Chem. Theory Comput. 13, 5552–5559 (2017).
- ⁷⁴Y. Hori, M. Nishida, F. Lim, T. Ida, and M. Mizuno, "Simulation of molecular Auger spectra using a two-electron Dyson propagator," J. Electron Spectrosc. Relat. Phenom. **207**, 60–64 (2016).
- ⁷⁵W. Skomorowski and A. I. Krylov, "Feshbach–Fano approach for calculation of Auger decay rates using equation-of-motion coupled-cluster wave functions. I. Theory and implementation," J. Chem. Phys. 154, 084124 (2021).
- ⁷⁶ A. K. Schnack-Petersen, T. Moitra, S. D. Folkestad, and S. Coriani, "New implementation of an equation-of-motion coupled-cluster damped-response framework with illustrative applications to resonant inelastic X-ray scattering," J. Phys. Chem. A 127, 1775–1793 (2023).
- $^{\bf 77}$ J. V. Ortiz, "Qualitative propagator theory of AX4 Auger spectra," J. Chem. Phys. $\bf 81,5873-5888$ (1984).
- ⁷⁸ J. V. Ortiz, "Qualitative propagator theory of CH₃CN, CH₃NC, and CH₃CCH Auger spectra," J. Chem. Phys. **83**, 4604–4617 (1985).
- ⁷⁹T. Ida and J. V. Ortiz, "Second-order, two-electron Dyson propagator theory: Comparisons for vertical double ionization potentials," J. Chem. Phys. **129**, 084105 (2008).
- 80 P. S. Bagus and H. F. Schaefer, "Localized and delocalized 1s hole states of the ${\rm O_2}^+$ molecular ion," J. Chem. Phys. **56**, 224–226 (1972).
- ⁸¹G. Wight and C. Brion, "K-shell excitations in NO and O₂ by 2.5 keV electron impact," J. Electron Spectrosc. Relat. Phenom. 4, 313–325 (1974).
- ⁸² J. T. Golab and D. L. Yeager, "The multiconfigurational spin-tensor electron propagator method for determining vertical principal and shake-up ionization potentials for open shell and highly correlated atoms and molecules," J. Chem. Phys. 87, 2925–2944 (1987).
- ⁸³D. Heryadi, D. L. Yeager, J. T. Golab, and J. A. Nichols, "Multiconfigurational spin tensor electron propagator vertical ionization potentials for O₂: Comparison to some other forefront methods using the same basis sets and geometries," J. Chem. Phys. 102, 9444–9445 (1995).
- ⁸⁴J. V. Ortiz, "Approximate Brueckner orbitals in electron propagator calculations," Int. J. Quantum Chem. 75, 615–621 (1999).
- 85 M. Ehara and H. Nakatsuji, "Outer- and inner-valence ionization spectra of N_2 and CO: SAC-CI (general-R) compared with full-CI spectra," Chem. Phys. Lett. **282**, 347–354 (1998).

- 86 I. Martín, A. Lavin, M. Velasco, M. Martin, J. Karwowski, and G. Diercksen, "Quantum defect orbital study of electronic transitions in Rydberg molecules: Ammonium and fluoronium radicals," Chem. Phys. 202, 307–320 (1996).
- ⁸⁷L. Yang, H. Ågren, V. Carravetta, and L. G. M. Pettersson, "Static exchange and quantum defect analysis of x-ray absorption spectra of carbonyl compounds," Phys. Scr. 54, 614 (1996).
- ⁸⁸ J. V. Ortiz, I. Martín, A. M. Velasco, and C. Lavín, "Ground and excited states of NH₄: Electron propagator and quantum defect analysis," J. Chem. Phys. **120**, 7949–7954 (2004).
- ⁸⁹W. Liu and D. Peng, "Exact two-component Hamiltonians revisited," J. Chem. Phys. 131, 031104 (2009).
- ⁹⁰M. Barysz and A. J. Sadlej, "Two-component methods of relativistic quantum chemistry: From the Douglas-Kroll approximation to the exact two-component formalism," J. Mol. Struct.: THEOCHEM 573, 181–200 (2001).
- ⁹¹ F. Pawłowski and J. V. Ortiz, "Relativistic electron detachment energies and spin-orbit splittings from quasiparticle electron propagator calculations," Mol. Phys. 118, e1700314 (2020).
- ⁹²L. A. Cunha, D. Hait, R. Kang, Y. Mao, and M. Head-Gordon, "Relativistic orbital-optimized density functional theory for accurate core-level spectroscopy," J. Phys. Chem. Lett. 13, 3438–3449 (2022).
- ⁹³ J. M. Kasper, T. F. Stetina, A. J. Jenkins, and X. Li, "Ab initio methods for L-edge x-ray absorption spectroscopy," Chem. Phys. Rev. 1, 011304 (2020).
- ⁹⁴ H. Ågren, L. Selander, J. Nordgren, C. Nordling, K. Siegbahn, and J. Müller, "X-ray spectra and core hole energy curves of some diatomic molecules," Chem. Phys. 37, 161–171 (1979).
- 95 J. Rubensson, L. Petersson, N. Wassdahl, M. Bäckström, J. Nordgren, O. M. Kvalheim, and R. Manne, "Radiative decay of multiply excited core hole states in $\rm H_2O$," J. Chem. Phys. 82, 4486–4491 (1985).
- ⁹⁶J.-E. Rubensson, N. Wassdahl, R. Brammer, and J. Nordgren, "Local electronic structure in simple alcohols studied in x-ray emission," J. Electron Spectrosc. Relat. Phenom. 47, 131–145 (1988).
- ⁹⁷P. Glans, R. E. L. Villa, Y. Luo, H. Agren, and J. Nordgren, "X-ray emission spectroscopy measurements of fluorine substituted methanes," J. Phys. B: At., Mol. Opt. Phys. 27, 3399 (1994).
- ⁹⁸L. O. Werme, J. Nordgren, H. Ågren, C. Nordling, and K. Siegbahn, "X-ray emission spectra of small molecules," Z. Phys. A: At. Nucl. 272, 131–141 (1975).
 ⁹⁹J. Nordgren, H. Agren, L. O. Werme, C. Nordling, and K. Siegbahn, "X-ray
- ⁹⁹J. Nordgren, H. Agren, L. O. Werme, C. Nordling, and K. Siegbahn, "X-ray emission spectra of NH₃ and N₂O," J. Phys. B: At. Mol. Phys. 9, 295 (1976).
 ¹⁰⁰R. Obaid, C. Buth, G. L. Dakovski, R. Beerwerth, M. Holmes, J. Aldrich,
- ¹⁰⁰R. Obaid, C. Buth, G. L. Dakovski, R. Beerwerth, M. Holmes, J. Aldrich, M.-F. Lin, M. Minitti, T. Osipov, W. Schlotter, L. S. Cederbaum, S. Fritzsche, and N. Berrah, "LCLS in—Photon out: Fluorescence measurement of neon using soft x-rays," J. Phys. B: At., Mol. Opt. Phys. **51**, 034003 (2018).
- ¹⁰¹ L. Pettersson, M. Backstrom, R. Brammer, N. Wassdahl, J. E. Rubensson, and J. Nordgren, "Nitrogen and oxygen K emission spectra of nitrous oxide," J. Phys. B: At. Mol. Phys. 17, L279 (1984).
- ¹⁰²R. Brammer, L. Pettersson, M. Bäckström, J. Nordgren, and C. Nordling, "The x-ray emission spectrum of gaseous ethene," Chem. Phys. Lett. **106**, 425–427 (1984).
- ¹⁰³ T. E. Meehan, J. McColl, and F. P. Larkins, "Theoretical X-ray emission spectra for the fluoromethane molecules following carbon *K*-shell ionization," J. Electron Spectrosc. Relat. Phenom. **73**, 283–292 (1995).

- ¹⁰⁴R. E. LaVilla, "Carbon and fluorine x-ray emission and fluorine *K* absorption spectra of the fluoromethane molecules, $CH_{4-n}F_n$ (0 ≤ n ≤ 4). II," J. Chem. Phys. 58, 3841–3848 (1973).
- ¹⁰⁵M. S. Banna, B. E. Mills, D. W. Davis, and D. A. Shirley, "X-ray photoemission molecular orbitals of hydrogen fluoride and the fluorinated methanes," J. Chem. Phys. 61, 4780–4786 (1974).
- ¹⁰⁶D. W. Davis, M. S. Banna, and D. A. Shirley, "Core-level binding-energy shifts in small molecules," J. Chem. Phys. **60**, 237–245 (1974).
- ¹⁰⁷V. D. Yumatov, A. V. Okotrub, L. N. Mazalov, V. N. Mit'kin, D. M. Tolstyakov, and S. V. Zemskov, "X-ray spectra and electronic structure of the F₂ molecule," J. Struct. Chem. 27, 157–159 (1986).
- ¹⁰⁸P. Weightman, T. D. Thomas, and D. R. Jennison, "KVV Auger spectrum of F₂: The importance of hole-hole correlation," J. Chem. Phys. **78**, 1652–1662 (1983).
- ¹⁰⁹M. Tronc, G. C. King, and F. H. Read, "Carbon K-shell excitation in small molecules by high-resolution electron impact," J. Phys. B: At. Mol. Phys. 12, 137–157 (1979).
- ¹¹⁰A. Hitchcock and C. Brion, "K-shell excitation spectra of CO, N₂ and O₂," J. Electron Spectrosc. Relat. Phenom. **18**, 1–21 (1980).
- 111 R. N. Sodhi and C. Brion, "Reference energies for inner shell electron energy-loss spectroscopy," J. Electron Spectrosc. Relat. Phenom. 34, 363–372 (1984).
- 112 R. Püttner, I. Dominguez, T. J. Morgan, C. Cisneros, R. F. Fink, E. Rotenberg, T. Warwick, M. Domke, G. Kaindl, and A. S. Schlachter, "Vibrationally resolved O 1s core-excitation spectra of CO and NO," Phys. Rev. A 59, 3415–3423 (1999).
- $^{113}\text{E}.$ Shigemasa, K. Ueda, Y. Sato, T. Sasaki, and A. Yagishita, "Symmetry-resolved K-shell photoabsorption spectra of free N $_2$ molecules," Phys. Rev. A 45, 2915–2921 (1992).
- ¹¹⁴Y. Ma, C. T. Chen, G. Meigs, K. Randall, and F. Sette, "High-resolution *K*-shell photoabsorption measurements of simple molecules," Phys. Rev. A **44**, 1848–1858 (1991).
- ¹¹⁵G. Wight and C. Brion, "K-shell excitation of CH₄, NH₃, H₂O, CH₃OH, CH₃OCH₃ and CH₃NH₂ by 2.5 keV electron impact," J. Electron Spectrosc. Relat. Phenom. **4**, 25–42 (1974).
- ¹¹⁶J. Schirmer, A. B. Trofimov, K. J. Randall, J. Feldhaus, A. M. Bradshaw, Y. Ma, C. T. Chen, and F. Sette, "K-shell excitation of the water, ammonia, and methane molecules using high-resolution photoabsorption spectroscopy," Phys. Rev. A 47, 1136–1147 (1993).
- ¹¹⁷K. C. Prince, L. Avaldi, M. Coreno, R. Camilloni, and M. d. Simone, "Vibrational structure of core to Rydberg state excitations of carbon dioxide and dinitrogen oxide," J. Phys. B: At., Mol. Opt. Phys. **32**, 2551 (1999).
- ¹¹⁸D. P. Chong, "Density functional theory calculation of K-shell excitation of nitrous oxide," Chem. Phys. Lett. 441, 209–212 (2007).
- 119 E. Rühl and A. Hitchcock, "Oxygen K-shell excitation spectroscopy of hydrogen peroxide," Chem. Phys. 154, 323–329 (1991).
- 120 R. E. LaVilla, "K α emission spectrum of gaseous N2," J. Chem. Phys. 56, 2345–2349 (1972).